IEEE Access
Multidisciplinary | Rapid Review | Open Access Journal

Received December 31, 2019, accepted January 21, 2020, date of publication January 30, 2020, date of current version February 7, 2020.

Digital Object Identifier 10.1109/ACCESS.2020.2970439

Joint Trajectory and Resource Optimization for UAV-Enabled Relaying Systems

QINBO CHEN
School of Systems Sciences and Engineering, Sun Yat-sen University, Guangzhou 510006, China
School of Electronics and Communication Engineering, Sun Yat-sen University, Shenzhen 518107, China

e-mail: chenqb6@mail2.sysu.edu.cn

This work was supported by the National Natural Science Foundation of China under Grant 11771460.

ABSTRACT Unmanned aerial vehicles (UAVs) have attracted attentions due to their mobility and high possibility of the line of sight (LoS) channel. We can fully use these two properties by carefully optimizing the UAVs' trajectories and cooperating with some facilities. A UAV working as a mobile relay now attracts many interests due to its low cost and reliable performance. In this paper, we study a relaying system, where a UAV works as an aerial mobile relay to help some ground base stations send information to ground users periodically by using time division multiple access (TDMA). We aim to maximize the minimum average user rate through solving a non-convex and information causality constraints involved problem by jointly optimizing the UAV trajectory, nodes scheduling, and power allocation to ensure the fairness among all users. Finally, we propose an efficient iterative algorithm to solve a derived mixed-integer non-convex optimization problem to achieve this target by using block coordinate descent (BCD) and successive convex approximation (SCA) methods and prove the convergence of our algorithm. Simulations show the effectiveness of our proposed algorithm, some useful trade-offs and insights about the structure of our optimized trajectory, and the influence of two widely used trajectory initialization methods.

INDEX TERMS Convex optimization, mobility control, nodes scheduling, power allocation, UAV relay.

I. INTRODUCTION

Unmanned aerial vehicles (UAVs) have been widely applied both in military surveillance and in civilian applications such as the security and rescue due to the development of modern electronics and software technologies [1]. Recently, in order to support the fast-growing data demand, UAVs have been considered as an innovative tool to complement the existing communication systems due to their mobility, favorable channel characteristics, and on-demand deployments. Fully utilizing the potential of UAVs can enhance the system performance and enable flexible communication networks [2].

In wireless cellular communication systems, applications about UAV communications can be categorized into two typical cases: 1) Cellular-enabled UAV communication, where UAVs can be seen as legal users served by ground base stations (GBSs), they can be used in the package delivery and reconnaissance. In reality, for UAVs in various missions, controlling them through GBSs can provide a more reliable, low-latency, and higher data rate service [3]; 2) UAV-assisted cellular communication, where UAVs can be applied as base stations or relays to enhance the communication system performance efficiently. In the second scenario, UAVs are widely used in emergencies (e.g., after a natural disaster) and hotspot areas. Nowadays, how to efficiently utilize the mobility of UAVs in these two cases attracts attentions due to the performance gain and some potential benefits that it produces.

In general, there are two lines of research that exploit the UAV mobility for the communication performance optimization. On one hand, we can optimize the quasi-static positions of some UAVs to cover small areas with low control complexity efficiently [4]–[8]. On the other hand, we can optimize the trajectories of UAVs to serve larger areas flexibly [9]–[23]. Various demands result in these two different research directions, both of which have their advantages and disadvantages. For the former, a quasi-static UAV is usually applied as an aerial base station or a relay to cover small areas [4]–[8]. Reference [4] optimizes a UAV's altitude to maximize the coverage performance on the ground. Reference [5] minimizes the number of UAVs and distributes

The associate editor coordinating the review of this manuscript and approving it for publication was Marco Martalo.

them with one type of spiral flight path to serve all users on the ground. Reference [6] uses the monotonic optimization method to get the optimal location of a UAV relay and resource allocation results, where the UAV works as a relay to serve multiple transmitter-receiver pairs. In [7], multiple UAVs serve as relays to connect ground users and a gateway node. It maximizes the minimum user rate by jointly optimizing UAVs' locations and all available resources. Reference [8] uses an amplify-and-forward (AF) UAV relay to ensure two-way communications between a GBS and users. It optimizes the location of the UAV and nodes' powers to maximize the sum rate of both uplink and downlink.

In the trajectory optimization, we can fully utilize the mobility of a UAV that the high freedom degree of a UAV lets itself move in the three-dimension (3D) space freely. Solutions of trajectory optimization problems can fully use this unique characteristic to enhance the overall performance of UAV-aided communication systems because a proper trajectory design can shorten the total flying distance and also the distances among all nodes. However, the trajectory optimization is challenging in reality. On one hand, it involves an infinite number of time-continuous variables to determine the location of a UAV. On the other hand, the working environment is changing with time, and it is hard to control the trajectory precisely to obtain the optimal performance. One usually approximates the location of a UAV through time or path discretization to simplify the trajectory optimization problem and then solve it with the acceptable complexity [9].

In this paper, we focus on a UAV-aided mobile relaying system. Firstly, in this system, a UAV is typically applied as a mobile relay with the limited mobility to provide wireless connectivity among users when direct links are not reliable [9]–[15]. In [9], a UAV works as a mobile relay to deliver data between a transmitter and a receiver to maximize the receiver rate. Its simulations show that the proposed algorithm based on a mobile relay outperforms the one with a traditional static relay. In [10], a mobile UAV relay with the decode-and-forward (DF) scheme serves two paired users. It shows a trade-off between the energy efficiency (EE) and spectrum efficiency (SE) of this system. Moreover, Reference [11] discusses the feasibility of a UAV relay network and does some experiments to show its effectiveness. References [12], [13] minimize the outage probability of a UAV relay network, where an AF and a DF UAV relay have been used to deliver data between two nodes. In [14], a mobile UAV relay delivers data from a transmitter to a receiver, and an eavesdropper exists. It maximizes the security rate by optimizing the UAV's trajectory and nodes' powers. Reference [15] studies a multi-hop UAV relaying system through optimizing the available resources among nodes and UAVs' trajectories to maximize the end-to-end throughput.

Secondly, to gain better mobility, significant research efforts have been devoted to addressing new challenges in the UAV trajectory optimization [16]–[23]. In [16], [17], a UAV circularly flies around a GBS, and the GBS serves nearby users while the UAV serves the rest users to maximize the throughput of all users by optimizing available resources and the UAV's trajectory. Reference [18] maximizes the EE of a UAV-aided cellular data offloading system with resource optimization. Reference [19] focuses on the trajectory optimization of a UAV relay, which is used to serve edge users of multiple cells. Reference [20] uses multiple UAVs to serve ground users and maximizes the minimum user rate by optimizing the UAVs' trajectories and available resources. In [21], a UAV works as a mobile relay to serve users in a variety of communication modes. It tries to minimize the total mission completion time with the quality of service requirements by optimizing the UAV's trajectory and resource allocation. In [22], a mobile UAV relay delivers data between two nodes, and other nodes use the same spectrum to communicate with each other by using the device-to-device (D2D) technique. It maximizes the sum rate of all nodes by optimizing the UAV's trajectory and nodes' powers. Reference [23] uses an AF UAV relay to deliver data among multiple user pairs. It maximizes the minimum paired user rate by jointly optimizing the UAV's trajectory and all available resources.

The aforementioned works in the position optimization do not involve any time-varying variable, which simplifies their problems, and then their problems may have some unique structures to be used, as shown in [6], [8]. When time-varying variables are involved, performing problem transformations to get more tractable optimization problems and then solving them will be more difficult since variables are coupled over time. Thus, algorithms in the position optimization only show some insights, but cannot be directly applied to our problem.

Moreover, references about trajectory optimization problems have been classified into two cases, according to UAVs' scopes of activities (mobility) in this paper. On one hand, the study on trajectory optimization problems with a limited mobility UAV, in end-to-end communication systems [9]–[15], is now classical in the literature. However, as far as multiple users are involved and the UAV aims to gain better mobility to enhance the system performance, the trajectory optimization problem will still be challenging. In multi-user networks, the flying trajectory of a UAV could be adjusted to maintain favorable communication links and fully utilize its own mobility due to the larger scope of activities. Better performance could also be achieved by jointly optimizing the UAV trajectory and available resources, such as nodes scheduling and power allocations, which has not been well studied yet.

On the other hand, owing to multiple users, the study of the information causality caused by backhaul links will be interesting and difficult, and then attracts our attentions. When a UAV aims to obtain better mobility, according to references [16]–[23], most of them do not consider backhaul links, due to the assumption that UAVs have fixed backhaul links related to GBSs by using millimeter-wave technologies. In practice, sustaining backhaul links has various technical difficulties since UAVs are difficult to own wireline

backhauls as conventional GBSs. Taking backhaul links into consideration makes our problem more practical.

In our problem with multiple different users, adaptive communication with dynamic links' resource allocations will be exploited along with the UAV trajectory design to enhance the communication performance, as discussed in recent works, such as [21]. Compared to [21] where users are equivalent, multiple nodes with different abilities (total available resources, heights, locations) are involved in our paper. Our problem will be more challenging due to the factors such as more complicated causality constraints caused by backhaul links with uneven loads, efficiently using all available resources according to the distributions of nodes, and utilizing the potential of a UAV's mobility.

In addition, to the best of our knowledge, all widely used trajectory initialization algorithms are mostly based on intuitive methods, such as traveling salesman problem (TSP) [21] and circle packing theory [20]. Many references have already shown the conciseness and effectiveness of these two methods when nodes are equivalent. However, their influences are still unknown when multiple nodes with different abilities are involved, which will be discussed in our paper.

In this paper, we consider a UAV-aided relaying system, where a UAV works as an aerial mobile DF relay to help some ground base stations send information to ground users periodically by using time division multiple access. The main contributions of this paper are summarized as follows:

- We formulate the problem, which maximizes the minimum average user rate by optimizing the power allocation, UAV trajectory, and nodes scheduling, subject to the constraints on the mobility of a UAV, limited resources, and the information causality. This problem is highly non-convex due to coupled variables, and information causality constraints caused by backhaul links with uneven loads. It is more complicated to be solved because nodes with different abilities (total available resources, heights, locations) are involved, and we need to balance loads among them efficiently.
- In order to solve this problem, firstly, we apply the time discretization method and relax the binary variables to get a more tractable non-convex optimization problem. Secondly, we decouple variables and reconstruct both information causality constraints and our original problem. Finally, we use block coordinate descent (BCD) and successive convex approximation (SCA) methods to solve this problem efficiently.
- Simulations show the effectiveness of our proposed algorithm compared to other benchmark schemes. Moreover, some useful trade-offs and insights about the structure of our optimized trajectory and the influence of two widely used trajectory initialization methods have also been discussed.

The rest of this paper is organized as follows. In Section II, we introduce the system model. The problem formulation and solution are illustrated in Section III and IV, respectively. The convergence analysis is provided in Section V. The trajectory initialization and simulation results are shown in Section VI. Finally, we conclude this paper in Section VII.

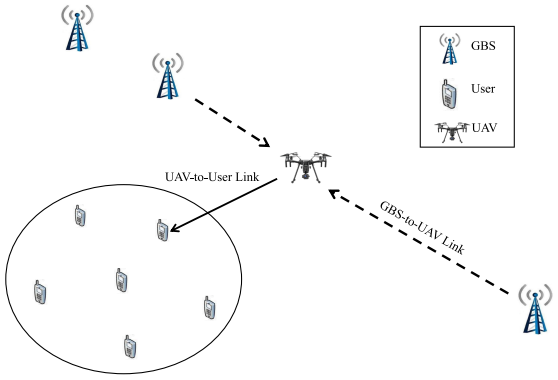

FIGURE 1. System model.

Notations: In this paper, scalars and vectors are denoted by italic letters and boldface lower-case letters, respectively. $\mathbb{R}^{M\times 1}$ denotes the space of M-dimensional real-valued vectors. $|\mathcal{K}|$ denotes the cardinality of a set $\mathcal{K}$. $\dot{\mathbf{q}}(t)$ represents the first-order derivative of a time-dependent function $\mathbf{q}(t)$. The Euclidean norm of a vector $\mathbf{a}$ is denoted by $||\mathbf{a}||$.

II. SYSTEM MODEL

In Fig.1, a UAV is employed as an aerial DF relay to help some ground base stations serve a group of K users on the ground periodically, and we assume that the UAV owns a data buffer of sufficiently large size and the Doppler effect caused by the mobility of the UAV can be well compensated at every receiver. Application scenarios include service recovery after an earthquake, military communication, and emergency communication [24]. To show possible insights and for clarity of exposition, we use the line of sight (LoS) channel model. Moreover, to ensure the high possibility of the LoS links, our system model is only valid for situations with few obstructs, such as rural areas, and a sufficiently high UAV [25].

The channels, between the UAV and other nodes in our problem, contain the LoS and non-line-of-sight (NLoS) components due to multi-path and shadowing effects. The free space path-loss model characterizes the LoS components. In general, there are two channel models to characterize the NLoS components. The first one is the probabilistic LoS channel model, where the probability of the air-to-ground LoS channel can be formulated as a function of elevation angles and environment parameters [26]. When the UAV is sufficiently high in open terrains, such as rural areas, the possibility of the LoS components will be large enough, and we can omit the NLoS components and only focus on the LoS components.

The second one is the Rician channel model, containing a Rician factor to represent the power ratio between the LoS components and the NLoS components. Reference [27] studies the relationship between the Rician factor and other variables, such as environment parameters

and the UAV-to-ground elevation angle. Reference [28] uses the angle-dependent Rician fading channel model, and the channel gain is related to the UAV-to-ground elevation angle. When the Rician factor or the elevation angle is large enough due to the proper UAV height and environment parameters, the LoS channel model is a reasonable approximation of the real channel. These discussions above suggest us to use the LoS channel model in our problem.

Our system model can be equivalently seen as a data dissemination system with backhaul links. Backhaul links are rarely considered in data dissemination systems, see for example [20]. In these systems, their system performance could be improved by allocating a part of backhaul links' resources to fronthaul links (data dissemination links) when fronthaul links lack resources. Moreover, our system model can be generalized to a similar scenario with multi-UAV, which can be solved by using our proposed algorithm with some modifications.

We assume that every GBS is far away from any user due to obstacles or the long distance, and that is why we need a UAV relay to deliver data. Moreover, we also assume every GBS has all required information, which means that we can get total data from any GBS to serve all users, and different GBSs should upload different parts of entire data to the UAV to get better system performance considering GBSs' distributions.

The user set is denoted by $\mathcal{K}$ with $|\mathcal{K}| = K$, and the GBS set is denoted by $\mathcal{L}$ with $|\mathcal{L}| = L$, and the UAV serves all nodes via a periodic time division multiple access (TDMA) with duration T. To show essential insights into the optimized trajectory, TDMA is more useful than dynamic frequency division multiple access (FDMA) [21] in our problem. We define the downlink direction as the direction from the UAV to a user and the uplink direction as the direction from a ground base station to the UAV. The proposed algorithm can be used in our model with a different uplink and downlink direction.

Without loss of generality, we consider a 3D Cartesian coordinate system where the horizontal coordinate of ground user k is denoted by $\mathbf{w}_k = [x_k, y_k]^T \in \mathbb{R}^{2\times 1}$, $k \in \mathcal{K} = \{1, 2, 3, \ldots, K\}$. A GBS's location is $\mathbf{b}_l = [x_{K+l}, y_{K+l}, H_G]^T \in \mathbb{R}^{3\times 1}$, $l \in \mathcal{L} = \{1, 2, 3, \ldots, L\}$ and every GBS's height is equal to H_G without loss of generality. The UAV flies at a fixed altitude H and its time-varying horizontal coordinate over time is $\mathbf{q}(t) = [x(t), y(t)]^T \in \mathbb{R}^{2\times 1}$.

The UAV needs to follow two constraints as below to keep itself safe and be ready for the next period

$$\mathbf{q}(0) = \mathbf{q}(T), \tag{1a}$$

$$||\dot{\mathbf{q}}(t)|| \le V_{\max}, \quad 0 \le t \le T. \tag{1b}$$

(1a) means that the UAV returns to its initial location at the end of every period to ensure that it flies periodically. The UAV speed is limited by $V_{\max}$ in (1b) for some security concerns. Moreover, the UAV's height H should also be carefully assigned according to some safety regulations, and it can ensure the high possibility of LoS links.

To handle time-continuous variables, we use the time discretization method to sample them with the sampling accuracy (slot length) $\delta_t = \frac{T}{N}$, where N is the number of sampling points (the total number of time slots). The slot length should be sufficiently small to keep the UAV approximately unchanged within any time slot, even at the maximum speed $V_{\max}$. However, in reality, we should balance the computation speed (complexity) and the precision to let our proposed algorithm be non-trivial, which will be explained in detail via simulation results in Section VI.

The UAV's positions $\mathbf{q}(t)$, $0 \le t \le T$, can be approximated by the sequences $\mathbf{q}[n] = [x[n], y[n]]^T, \forall n = \{1, \ldots, N\}$ and constraints (1a) and (1b) can be equivalently written as

$$\mathbf{q}[1] = \mathbf{q}[N], \tag{2a}$$

$$||\mathbf{q}[n+1] - \mathbf{q}[n]||^2 \le S_{\max}^2, \quad n = \{1, 2, \ldots, N-1\}. \tag{2b}$$

where $S_{\max} \triangleq V_{\max}\delta_t$ is the maximum horizontal distance that the UAV can fly within a time slot.

We assume that every user's location has been known, and the distance from the UAV to user k (3a) and from GBS l to the UAV (3b) at time slot n can be expressed as

$$D_k[n] = \sqrt{H^2 + ||\mathbf{q}[n] - \mathbf{w}_k||^2}, \quad \forall k, n, \tag{3a}$$

$$d_l[n] = \sqrt{(H - H_G)^2 + ||\mathbf{q}[n] - \mathbf{b}_l||^2}, \quad \forall l, n. \tag{3b}$$

The channel power gains, from the UAV to user k (4a) and from GBS l to the UAV (4b) at every time slot n, follow the free space path-loss model (the LoS channel model) and can be expressed as

$$H_k[n] = \rho_0 D_k^{-2}[n] = \frac{\rho_0}{H^2 + ||\mathbf{q}[n] - \mathbf{w}_k||^2}, \quad \forall k, n, \tag{4a}$$

$$h_l[n] = \rho_0 d_l^{-2}[n] = \frac{\rho_0}{||H - H_G||^2 + ||\mathbf{q}[n] - \mathbf{b}_l||^2}, \quad \forall l, n. \tag{4b}$$

where ρ_0 denotes the channel power gain at the reference distance $d_0 = 1$ m.

All nodes work in the half-duplex mode, which means that only one of total uplinks and downlinks can be activated per time slot at most. We define the binary variables $\alpha_k[n]$ and $\beta_l[n]$ in the following way: if user k or GBS l is served by the UAV at time slot n, $\alpha_k[n] = 1$ or $\beta_l[n] = 1$; otherwise, $\alpha_k[n] = 0$ or $\beta_l[n] = 0$. Therefore, we have the following two constraints

$$\sum_{k=1}^{K} \alpha_k[n] + \sum_{l=1}^{L} \beta_l[n] \le 1, \quad \forall k, l, n, \tag{5a}$$

$$\{\alpha_k[n], \beta_l[n]\} \in \{0, 1\}, \quad \forall k, l, n. \tag{5b}$$

Denote the transmission power of the UAV by $P_{\mathrm{r}}[n]$ at time slot n. If user k is scheduled for communication at time slot n, the maximum achievable rate of user k at time slot n in bits/second/Hz (bps/Hz) can be expressed as

$$R_k[n] = \log_2\left(1 + \frac{P_{\mathrm{r}}[n]H_k[n]}{\sigma^2}\right) = \log_2\left(1 + \frac{P_{\mathrm{r}}[n]\gamma_0}{H^2 + ||\mathbf{q}[n] - \mathbf{w}_k||^2}\right). \tag{6}$$

where σ^2 is the additive white Gaussian noise (AWGN) power at user k, which is assumed to be identical for every receiver, and $\gamma_0 \triangleq \frac{\rho_0}{\sigma^2}$ denotes the received reference signal-to-noise ratio (SNR) at $d_0 = 1$ m. Thus, the average achievable rate of user k over N time slots is given by

$$R_k = \frac{1}{N}\sum_{n=1}^{N}\alpha_k[n]R_k[n] = \frac{1}{N}\sum_{n=1}^{N}\alpha_k[n]\log_2\left(1+\frac{P_{\mathrm{r}}[n]\gamma_0}{H^2+||\mathbf{q}[n]-\mathbf{w}_k||^2}\right). \quad (7)$$

Denote the transmission power of GBS l by $P_{\mathrm{s}}^l[n]$ at time slot n. If GBS l is scheduled for communication at time slot n, the maximum achievable rate of the UAV that comes from GBS l at time slot n in bits/second/Hz (bps/Hz) can be expressed as

$$r_l[n] = \log_2\left(1+\frac{P_{\mathrm{s}}^l[n]h_l[n]}{\sigma^2}\right) = \log_2\left(1+\frac{P_{\mathrm{s}}^l[n]\gamma_0}{||H-H_G||^2+||\mathbf{q}[n]-\mathbf{b}_l||^2}\right). \quad (8)$$

Thus, the average achievable rate of the UAV that comes from GBS l over N time slots is given by

$$r_l = \frac{1}{N}\sum_{n=1}^{N}\beta_l[n]r_l[n] = \frac{1}{N}\sum_{n=1}^{N}\beta_l[n]\log_2\left(1+\frac{P_{\mathrm{s}}^l[n]\gamma_0}{||H-H_G||^2+||\mathbf{q}[n]-\mathbf{b}_l||^2}\right). \quad (9)$$

We use two constraints as follows to limit every GBS's and the UAV's transmission power through the average power constraint (10a) and the peak power constraint (10b)

$$\frac{1}{N}\sum_{n=1}^{N}P_{\mathrm{s}}^l[n] \le P_{\mathrm{s}}^{\mathrm{ave}}, \quad \frac{1}{N}\sum_{n=1}^{N}P_{\mathrm{r}}[n] \le P_{\mathrm{r}}^{\mathrm{ave}}, \ \forall\, l, n, \quad (10a)$$

$$0 \le P_{\mathrm{s}}^l[n] \le P_{\mathrm{s}}^{\max}, \quad 0 \le P_{\mathrm{r}}[n] \le P_{\mathrm{r}}^{\max}, \ \forall\, l, n. \quad (10b)$$

Usually, the average power is smaller than the peak power to make these power constraints non-trivial.

III. PROBLEM FORMULATION

Let $\mathbf{A} = \{\alpha_k[n], \beta_l[n], \forall\, k, l, n\}$, $\mathbf{Q} = \{\mathbf{q}[n], \forall\, n\}$, $\mathbf{P} = \{P_{\mathrm{s}}^l[n], P_{\mathrm{r}}[n], \forall\, l, n\}$. Our goal is to maximize the minimum (max-min) average user rate among all users (for fairness) by optimizing the nodes scheduling $\mathbf{A}$, UAV trajectory $\mathbf{Q}$, and nodes' powers $\mathbf{P}$. The optimization problem is formulated as

$$\max_{\mathbf{A},\mathbf{Q},\mathbf{P}} \ \min R_k$$

$$\text{s.t.} \ \sum_{l=1}^{L} r_l \ge \sum_{k=1}^{K} R_k, \quad (11a)$$

$$(2a), (2b), (5a), (5b), (10a), (10b). \quad (11b)$$

Reference [21] gives different thresholds to different transmitter and receiver pairs to ensure that information causality constraints can be met in a periodic operation scenario. In other words, for the k-th user in the transmitter set, its time-average rate, from itself to the UAV, is equal to the time-average rate between the UAV and the k-th user in the receiver set. If every paired transmitter and receiver can meet this condition, the loose information causality can be achieved.

The loose information causality in our model means that the transmitted information should be larger than or at least equal to the received information for the UAV within the given flying time T rather than at every time slot. The reason is that the UAV may relay some information that it received before, and this assumption can make our optimization problem more tractable. In our problem, we use constraint (11a) to ensure the loose information causality, which means that the total data transmitted by all GBSs should be larger than or at least equal to the entire data sent by the UAV within the time T.

We introduce a slack variable η for constraint (11a) and rewrite it as (12a) and (12b), and then problem (11) can be rewritten as

$$\max_{\mathbf{A},\mathbf{Q},\mathbf{P}} \ \eta$$

$$\text{s.t.} \ \frac{1}{N}\sum_{n=1}^{N}\alpha_k[n]\log_2\left(1+\frac{P_{\mathrm{r}}[n]\gamma_0}{H^2+||\mathbf{q}[n]-\mathbf{w}_k||^2}\right) \ge \eta, \quad \forall\, k, \quad (12a)$$

$$\frac{1}{N}\sum_{l=1}^{L}\sum_{n=1}^{N}\beta_l[n]\log_2\left(1+\frac{P_{\mathrm{s}}^l[n]\gamma_0}{||H-H_G||^2+||\mathbf{q}[n]-\mathbf{b}_l||^2}\right) \ge K\eta, \quad (12b)$$

$$(11b). \quad (12c)$$

Problems (11) and (12) are equivalent since (11a) is equivalent to constraints (12a) and (12b) at the optimal solution. The reason is that these three constraints must be met with equalities at the optimal solution; otherwise, we can do resource reallocation to get a better solution. Even though some user channel is better due to the shorter distance to the UAV and can support a higher user rate, we still reduce its allocated resources and reallocate them to worse users, and then every user rate should be equal to η, to maximize the minimum average user rate and to ensure the fairness.

The main difficulties for this problem are due to the fact that variables $\mathbf{A}$, $\mathbf{Q}$, and $\mathbf{P}$ are coupled, and the fact that the left-hand-side (LHS) of (12a) and (12b) are not concave. Moreover, constraint (5b) involves integers which make problem (12) hard to handle. Furthermore, for the given UAV trajectory, problem (12) is still not convex with respect to $\mathbf{A}$ and $\mathbf{P}$. Therefore, problem (12) is a mixed-integer non-convex problem, and it is hard to find its optimal solution in general.

IV. SOLUTION

To solve problem (12), we first relax the binary variables in (5b) into continuous variables to get the following problem

$$\max_{\mathbf{A},\mathbf{Q},\mathbf{P}} \quad \eta$$
$$\text{s.t. } 0 \le \alpha_k[n], \quad \beta_l[n] \le 1, \ \forall k, l, n, \tag{13a}$$
$$\text{(2a), (2b), (5a), (10a), (10b), (12a), (12b).} \tag{13b}$$

Problem (13) is the upper bound of (12) due to the relaxation of the binary variables. Firstly, for the given UAV trajectory, the nodes scheduling and power allocation problem in (13) can be solved by CVX (a Matlab-based modeling system for convex optimization), respectively. Secondly, for the given resource allocation result, the trajectory optimization problem is still non-convex due to the non-convexity of constraints involving the UAV's positions in (13). Therefore, we apply block coordinate descent and successive convex approximation methods to solve the relaxed problem (13).

A. NODES SCHEDULING

For any given UAV trajectory $\mathbf{Q}$ and power allocation $\mathbf{P}$, problem (13) is simplified as

$$\max_{\mathbf{A}} \quad \eta$$
$$\text{s.t. } \frac{1}{N}\sum_{n=1}^{N}\alpha_k[n]\log_2\left(1+\frac{P_{\mathrm{r}}[n]\gamma_0}{H^2+||\mathbf{q}[n]-\mathbf{w}_k||^2}\right) \ge \eta, \ \forall k, \tag{14a}$$
$$\frac{1}{N}\sum_{l=1}^{L}\sum_{n=1}^{N}\beta_l[n]\log_2\left(1+\frac{P_{\mathrm{s}}^{l}[n]\gamma_0}{||H-H_G||^2+||\mathbf{q}[n]-\mathbf{b}_l||^2}\right) \ge K\eta, \tag{14b}$$
$$\sum_{k=1}^{K}\alpha_k[n]+\sum_{l=1}^{L}\beta_l[n] \le 1, \quad \forall k, l, n, \tag{14c}$$
$$0 \le \alpha_k[n], \beta_l[n] \le 1, \quad \forall k, l, n. \tag{14d}$$

It's a convex optimization problem. We can use CVX to solve it directly [29]. All constraints in problem (14) must be met with equalities; otherwise, we can always reallocate unused resources to get a better η.

B. TRAJECTORY OPTIMIZATION

For any given nodes scheduling $\mathbf{A}$ and power allocation $\mathbf{P}$, the trajectory optimization problem can be solved by using SCA and be written as

$$\max_{\mathbf{Q}} \quad \eta$$
$$\text{s.t. (2a), (2b), (14a), (14b).} \tag{15}$$

Problem (15) is not convex with respect to the variable $\mathbf{q}[n]$. However, it is a convex optimization problem of $||\mathbf{q}[n]-\mathbf{w}_k||^2$ and $||\mathbf{q}[n]-\mathbf{b}_l||^2$ since the LHS of constraints (14a) and (14b) are convex functions of these two quantities. From [30], the first-order Taylor expansion of a convex function is its global lower bound at any point, and then we can apply SCA for all $R_k[n]$ and $r_l[n]$ to get lower bounds of them

$$R_k[n] = \log_2\left(1+\frac{P_{\mathrm{r}}[n]\gamma_0}{H^2+||\mathbf{q}[n]-\mathbf{w}_k||^2}\right)$$
$$\ge -A_k^r[n]\left(||\mathbf{q}[n]-\mathbf{w}_k||^2-||\mathbf{q}^r[n]-\mathbf{w}_k||^2\right)+B_k^r[n] \tag{16a}$$
$$\triangleq R_k^{lb,r}[n], \tag{16b}$$

where

$$t_k^r[n] = H^2+||\mathbf{q}^r[n]-\mathbf{w}_k||^2+P_{\mathrm{r}}[n]\gamma_0, \quad \forall k, n, \tag{17a}$$
$$A_k^r[n] = \frac{P_{\mathrm{r}}[n]\gamma_0\log_2 e}{(H^2+||\mathbf{q}^r[n]-\mathbf{w}_k||^2)t_k^r[n]}, \quad \forall k, n, \tag{17b}$$
$$B_k^r[n] = \log_2\left(1+\frac{P_{\mathrm{r}}[n]\gamma_0}{H^2+||\mathbf{q}^r[n]-\mathbf{w}_k||^2}\right), \quad \forall k, n. \tag{17c}$$

Each $r_l[n]$ has a similar lower bound $r_l^{lb,r}[n]$, and we refer interested readers to [9] for a proof of SCA.

We now have convex optimization problem (18) based on these lower bounds, which can be solved by CVX [29].

$$\max_{\mathbf{Q}} \ \eta^{lb,r}$$
$$\text{s.t. } \frac{1}{N}\sum_{n=1}^{N}\alpha_k[n]R_k^{lb,r}[n] \ge \eta^{lb,r}, \quad \forall k, \tag{18a}$$
$$\frac{1}{N}\sum_{l=1}^{L}\sum_{n=1}^{N}\beta_l[n]r_l^{lb,r}[n] \ge K\eta^{lb,r}, \tag{18b}$$
$$\mathbf{q}[1] = \mathbf{q}[N], \tag{18c}$$
$$||\mathbf{q}[n+1]-\mathbf{q}[n]||^2 \le S_{\max}^2, \quad n = \{1, 2, \ldots, N-1\}. \tag{18d}$$

C. POWER ALLOCATION

For any given nodes scheduling $\mathbf{A}$ and UAV trajectory $\mathbf{Q}$, the power allocation problem can be written as

$$\max_{\mathbf{P}} \quad \eta$$
$$\text{s.t. } \frac{1}{N}\sum_{n=1}^{N}\alpha_k[n]\log_2\left(1+\frac{P_{\mathrm{r}}[n]\gamma_0}{H^2+||\mathbf{q}[n]-\mathbf{w}_k||^2}\right) \ge \eta, \quad \forall k, \tag{19a}$$
$$\frac{1}{N}\sum_{l=1}^{L}\sum_{n=1}^{N}\beta_l[n]\log_2\left(1+\frac{P_{\mathrm{s}}^{l}[n]\gamma_0}{||H-H_G||^2+||\mathbf{q}[n]-\mathbf{b}_l||^2}\right) \ge K\eta, \tag{19b}$$
$$\frac{1}{N}\sum_{n=1}^{N}P_{\mathrm{s}}^{l}[n] \le P_{\mathrm{s}}^{\mathrm{ave}}, \quad \frac{1}{N}\sum_{n=1}^{N}P_{\mathrm{r}}[n] \le P_{\mathrm{r}}^{\mathrm{ave}}, \ \forall l, n, \tag{19c}$$
$$0 \le P_{\mathrm{s}}^{l}[n] \le P_{\mathrm{s}}^{\max}, \quad 0 \le P_{\mathrm{r}}[n] \le P_{\mathrm{r}}^{\max}, \quad \forall l, n. \tag{19d}$$

It's also a convex optimization problem that can be solved by CVX [29]. Since every GBS's power is usually larger than the UAV's power, we can use some tricks to re-optimize the optimized power allocation results. If a GBS's power is large enough, there must be some unused energy left.

Through observations, CVX tends to randomly distribute some of them at some time slots, where we do not schedule the GBS. Therefore, the power allocated at these unscheduled time slots can be set to be zero directly to save energy for other purposes. If there are some eavesdroppers, every GBS can use its unused energy to send jamming signals to enhance the system security at its unscheduled time slots.

Algorithm 1 Block Coordinate Descent Algorithm for Problem (13).

1: Trajectory and Power Allocation Initialization: $\mathbf{Q}^0$ and $\mathbf{P}^0$.
2: **repeat**
3: For the given $\mathbf{Q}^r$ and $\mathbf{P}^r$, we solve problem (14) to get the updated $\mathbf{A}^{r+1}$.
4: For the given $\mathbf{A}^{r+1}$ and $\mathbf{P}^r$, we solve problem (18) to get the updated $\mathbf{Q}^{r+1}$.
5: For the given $\mathbf{A}^{r+1}$ and $\mathbf{Q}^{r+1}$, we solve problem (19) to get the updated $\mathbf{P}^{r+1}$.
6: Update $r = r + 1$.
7: **until** The fractional increase of the objective value is less than or equal to a small threshold ϵ.

V. CONVERGENCE ANALYSIS

We define $\eta_{\text{sch}}(\mathbf{A}^{r+1}, \mathbf{Q}^r, \mathbf{P}^r)$, $\eta_{\text{tra}}(\mathbf{A}^{r+1}, \mathbf{Q}^{r+1}, \mathbf{P}^r)$, and $\eta_{\text{pow}}(\mathbf{A}^{r+1}, \mathbf{Q}^{r+1}, \mathbf{P}^{r+1})$ as the $(k+1)$-th objective value of problems (14), (15), and (19) based on the k-th iteration result ($\mathbf{A}^r$, $\mathbf{Q}^r$, and $\mathbf{P}^r$), respectively. Moreover, $\eta_{\text{tra}}^{lb,r}(\mathbf{A}^{r+1}, \mathbf{Q}^{r+1}, \mathbf{P}^r)$ is the objective value of problem (18) with the help of SCA, and $\eta(\mathbf{A}^r, \mathbf{Q}^r, \mathbf{P}^r)$ is the objective value of problem (13) based on the k-th iteration result.

Since both (14) and (19) are convex optimization problems already, we have

$$\eta_{\text{sch}}(\mathbf{A}^{r+1}, \mathbf{Q}^r, \mathbf{P}^r) \geq \eta(\mathbf{A}^r, \mathbf{Q}^r, \mathbf{P}^r) \quad (20)$$
$$= \eta_{\text{pow}}(\mathbf{A}^r, \mathbf{Q}^r, \mathbf{P}^r), \quad (21)$$
$$\eta_{\text{pow}}(\mathbf{A}^{r+1}, \mathbf{Q}^{r+1}, \mathbf{P}^{r+1}) \geq \eta(\mathbf{A}^{r+1}, \mathbf{Q}^{r+1}, \mathbf{P}^r), \quad (22)$$
$$\eta(\mathbf{A}^{r+1}, \mathbf{Q}^{r+1}, \mathbf{P}^{r+1}) = \eta_{\text{pow}}(\mathbf{A}^{r+1}, \mathbf{Q}^{r+1}, \mathbf{P}^{r+1}). \quad (23)$$

Moreover, since we apply SCA for problem (15), we have

$$\eta(\mathbf{A}^{r+1}, \mathbf{Q}^{r+1}, \mathbf{P}^r) \geq \eta_{\text{tra}}^{lb,r}(\mathbf{A}^{r+1}, \mathbf{Q}^{r+1}, \mathbf{P}^r) \quad (24)$$
$$\geq \eta_{\text{tra}}^{lb,r}(\mathbf{A}^{r+1}, \mathbf{Q}^r, \mathbf{P}^r) \quad (25)$$
$$= \eta_{\text{sch}}(\mathbf{A}^{r+1}, \mathbf{Q}^r, \mathbf{P}^r). \quad (26)$$

(20) is due to the optimization of nodes scheduling for the given $\mathbf{Q}^r$ and $\mathbf{P}^r$. (22) and (25) have similar reasons. Furthermore, (24) can be derived from the fact that the objective value of (18) is a lower bound.

Based on all inequalities above, we obtain

$$\eta(\mathbf{A}^{r+1}, \mathbf{Q}^{r+1}, \mathbf{P}^{r+1}) \geq \eta(\mathbf{A}^r, \mathbf{Q}^r, \mathbf{P}^r), \quad (27)$$
$$\eta_{\text{pow}}(\mathbf{A}^{r+1}, \mathbf{Q}^{r+1}, \mathbf{P}^{r+1}) \geq \eta_{\text{tra}}^{lb,r}(\mathbf{A}^{r+1}, \mathbf{Q}^{r+1}, \mathbf{P}^r) \quad (28)$$
$$\geq \eta_{\text{sch}}(\mathbf{A}^{r+1}, \mathbf{Q}^r, \mathbf{P}^r) \quad (29)$$
$$\geq \eta_{\text{pow}}(\mathbf{A}^r, \mathbf{Q}^r, \mathbf{P}^r). \quad (30)$$

Therefore, objective values of (14), (18), (19), and the relaxed problem (13) are non-decreasing and will converge to a finite value, which is strictly less than $\frac{1}{K}\log_2\left(1+\frac{P_{\text{r}}^{\max}\gamma_0}{H^2}\right)$(bps/Hz).

VI. TRAJECTORY INITIALIZATION AND SIMULATION RESULTS

In this section, we discuss trajectory initialization methods and simulation results.

A. TRAJECTORY INITIALIZATION

We need to find an efficient trajectory initialization method to start algorithm 1. There are two widely used trajectory initialization methods; one is based on the circle packing scheme [20], and the other is based on the TSP [21]. The former is better in our problem because the TSP method does not distinguish the abilities (such as total available resources, heights, locations) of various transmitters. Our model can be equivalently seen as a model that both GBSs and users try to send information to the UAV. If a GBS works as a transmitter, it shows the advantages of the higher power and the better channel gain, and the better channel gain is due to its fixed height compared to any ground user. From this viewpoint, the imposed fairness assumption of the TSP method is not suitable for our problem, and the simulation results in Fig.5 justifies this conclusion.

To use the circular initial trajectory, we define the geometric center of users as $C = \frac{\sum_k \mathbf{w}_k}{K}$. A half of the radius of a circle, which is centered at C and can cover all users, is $r_1 = \frac{1}{2} * \max_k ||\mathbf{w}_k - C||, \forall\, k$ (balancing the number of users inside and outside the circle, and abandoning all far away GBSs to ensure that r_1 is non-trivial). The maximum allowed radius is $r_2 = \frac{V_{\max}T}{2\pi}$ for a given T. Thus, the radius of our required circle is $r = \min\{r_1, r_2\}$ and the UAV initial trajectory is $Q^r[n] = [C + r\cos\theta_n, C + r\sin\theta_n]^T, \forall\, n$, where $\theta_n = \frac{2\pi}{N-1} * (n-1)$.

As far as the TSP based initial trajectory is concerned, firstly, one solves a traveling salesman problem to get the minimum traveling time T_{th}, which the UAV spends on visiting all nodes, and the TSP optimal visiting order. For any given time T, when $T \leq T_{th}$, there are some waypoints (virtual points) which stay around their associated nodes. When we minimize the distances among all waypoints, the distance between any waypoint and its associated node should be less than or at most equal to a value r, which will be minimized simultaneously. One uses the optimized path among all waypoints as the initial trajectory. When $T > T_{th}$, the UAV visits all nodes according to the TSP optimal visiting order and spends a part of T to stay at the top of all nodes. We refer the interested reader to [21] for details regarding the TSP based initial trajectory.

B. SIMULATION RESULTS

We use parameters in Table 1, the distributions of users and GBSs in Fig.2, and the circular initial trajectory as the basic settings, unless otherwise specified.

TABLE 1. Parameters for numerical simulations.

UAV altitude	$H = 100$ m
GBS altitude	$H_G = 20$ m
Maximum UAV speed	$V_{\max} = 50$ m/s
Channel power gain at d_0=1 m	$\gamma_0 = -60$ dB
AWGN power	$\delta^2 = -110$ dBm
Simulation threshold	$\epsilon = 10^{-3}$
Average power of every GBS	$P_{\rm s}^{\rm ave} = 1W$
Average power of the UAV	$P_{\rm r}^{\rm ave} = 0.02W$
Peak power of every GBS	$P_{\rm s}^{\max} = 5W$
Peak power of the UAV	$P_{\rm r}^{\max} = 0.1W$
Number of users	6
Number of GBSs	3

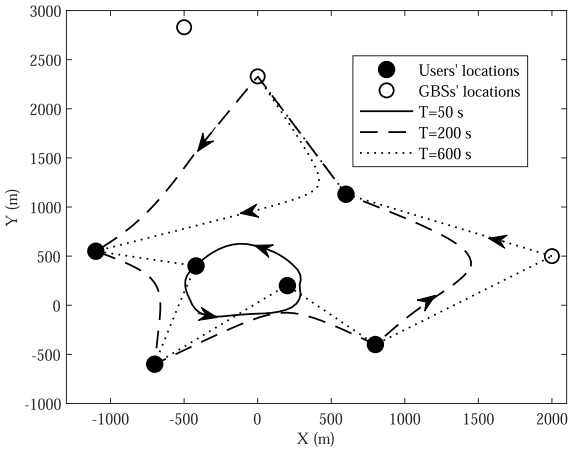

FIGURE 2. The optimized UAV trajectory for different flying time T.

In our simulation, we use six users and three GBSs. Distributions of GBSs can be classified into two typical cases. 1) Clustered GBS, the distance between any two GBSs within one cluster is less than or at most equal to a specified value. 2) Isolated GBS, a GBS which is far away from all other GBSs. Therefore, we use three GBSs to simulate these two types of distributions to get more general results.

As for users, when the number of them is too small, the optimized trajectory will be too simple to show insights, and it also changes slowly with the increasing T. If the number of users is too large, similar results show up. The simulation speed will also decrease even if T is small because each node needs enough memory resources to represent its status at every time slot. When the number of users is suitable, the influence of T can be demonstrated more clearly with the acceptable computation speed. Therefore, it is reasonable to select six users and three GBSs to construct a suitable flight area for the UAV considering the CVX (a Matlab-based modeling system for convex optimization) computation ability.

Fig.2 shows that the UAV trajectory changes with the mission completion time T. When T is small, the UAV trajectory will be limited over a small scale; otherwise, completing a too long trajectory within a given time T will be our main objective, and the max-min average user rate will compromise with this new objective, which is not worthwhile. Therefore, there

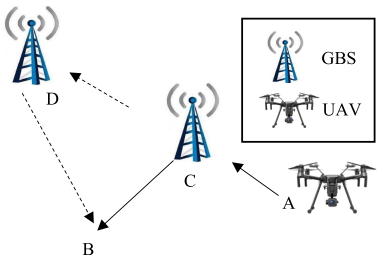

FIGURE 3. An illustration of different UAV trajectories.

is a trade-off when T is small. When the UAV flies closer to any GBS, the distance between itself and any user will increase, and most of the available resources will be allocated to users, but this still leads to a smaller η since T is small (flying closer to GBSs wasting precious time) and the distance between the UAV and users increases. If the UAV tries to fly closer to users, a similar phenomenon also shows up. The optimized trajectory should balance the distance among all nodes, and also be careful of the total flying distance, which leads to a reasonable resource allocation result and a larger η.

When T increases, the UAV also expands its scope of activities. In Fig.2, when T is large enough, the UAV stops at the top of all users to get the best LoS channel to increase the max-min average user rate. However, the UAV may not need to stay at the top of every GBS to get the best UAV-GBS link gain and then to achieve a possible better solution with a limited T. This phenomenon produces another trade-off in our work, whether the cost spend, when the UAV flies closer to a GBS, can be compensated by the better UAV-GBS link gain or not. We will explain it in the following example. In Fig.3, when the UAV flies from A to B, there are two paths with equal flying time. The path which the UAV flies from A, C, to B is named as path 1, and the time during which it spends for staying at the top of C to receive data from C and D is named as T_1. Moreover, the UAV also flies from A, C, D, to B, which is named as path 2, and it will spend part of T_1 to complete this path. Under this assumption, in path 2, the cost is that the UAV spends more time flying, and it receives fewer data from C. However, the better link gain between the UAV and D will provide more data to compensate the cost either partially or entirely depending on the location and the power supply of D. Therefore, if the cost can be offset, the UAV will fly closer to D and may stay at the top of it; otherwise, the priority of GBS D's location in the optimized trajectory will go down due to the limited time T, but the UAV may still receive some data from it due to the limited power supply of every GBS.

In Fig.2 and Fig.4, the UAV stays at the top of every user and some GBSs to get the best LoS channel and then flies among them at the maximum speed to avoid wasting time when T = 600s; otherwise, we can always increase the UAV speed to save time, and then reallocate it to get a better η. On one hand, when T or V $\rightarrow \infty$, we can omit the UAV flying time and solve a TSP to find the shortest path among

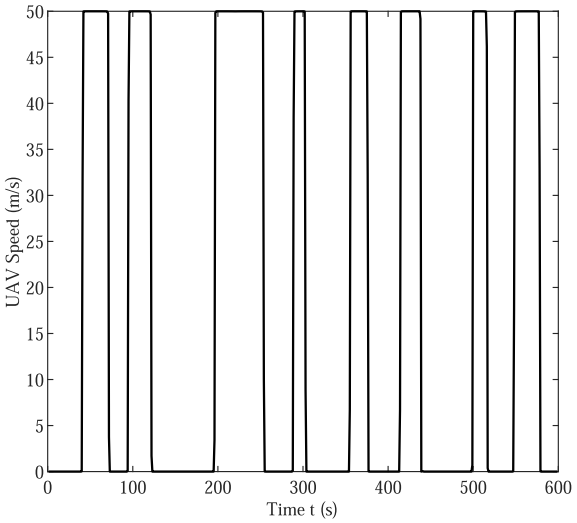

FIGURE 4. The UAV speed versus time t when T = 600s.

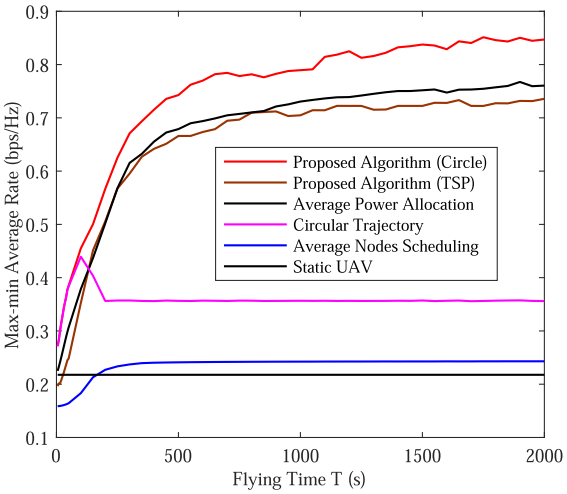

FIGURE 5. The max-min average user rate versus flying time T.

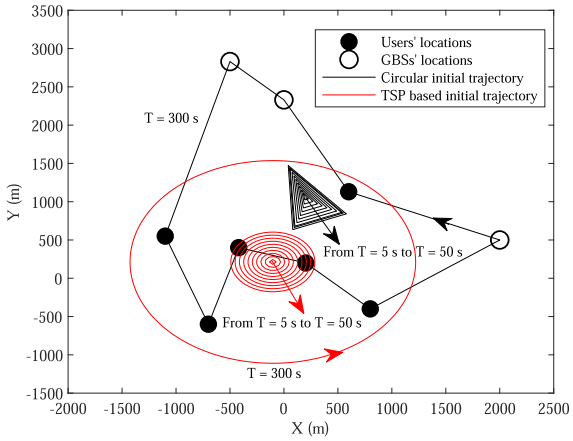

FIGURE 6. The initial trajectory of the TSP based method and the circle packing theory based method.

all ground nodes, which is the optimal trajectory. On the other hand, if we do not consider the average power constraint of every GBS and then let T or V $\rightarrow \infty$, we can select one of GBSs as the only GBS to reconstruct our problem and get an equivalently optimal solution.

Fig.5 shows the comparison among different algorithms. 1) **Our proposed algorithm (Circle)**, algorithm 1 with the circular initial trajectory. 2) **Our proposed algorithm (TSP)**, algorithm 1 with the TSP based initial trajectory. 3) **Average power allocation algorithm**, we use the average power of every GBS and the UAV at every time slot, and then we do the nodes scheduling and trajectory optimization. 4) **Circular trajectory algorithm**, we use the circular UAV trajectory, and then do the power allocation and nodes scheduling optimization. 5) **Average nodes scheduling algorithm**, the UAV communicates with all users and GBSs at every time slot, and then we do the power allocation and trajectory optimization. 6) **Static UAV algorithm**, the UAV stays static at the geometric center of all users, and then we optimize other variables. Algorithms 3 - 5 use the circular initial trajectory.

In Fig.5, algorithm 1 outperforms other five algorithms. The imposed fairness assumption of the TSP based trajectory initialization method in algorithm 2 is not suitable for our problem, and it then leads to the degraded performance compared with algorithm 1. Moreover, in Fig.6, when T is small, the TSP based initial trajectory is closer to GBSs compared to the circular one, and the UAV will be also closer to GBSs. This induces a smaller η since T is small (flying closer to GBSs wasting precious time) and the distance between the UAV and users increases. When T is not large enough, such as 300s in Fig.6, the TSP based initial trajectory tends to visit all nodes. This will degrade the system performance due to the same reason shown in Fig.3. When T is large enough and the UAV tends to visit all nodes, the TSP optimal visiting order could not be the optimal result and also affect the optimized trajectory. This phenomenon also degrades the performance. In this sense, the initial trajectory based on the circle packing theory is much better in our problem.

Drawbacks of algorithm 3 are mainly due to two reasons. Firstly, the uniformly distributed GBSs' powers lead to wasting energy. Even if the total power of every GBS is much larger than that of the UAV, the wasted energy still degenerates our system performance. However, the influence of wasting GBSs' powers may be less severe and not the main reason since the impact of uniformly allocating the UAV power is much more significant, and a fraction of GBSs' total powers means being unused, even at the optimal solution. Secondly, algorithm 3 cannot thoroughly use the precious UAV power, and this leads to the result that the optimized trajectory compromises with the pre-allocated UAV power. Moreover, the max-min average user rate of algorithm 4 firstly increases, and then decreases after it achieves its peak, and finally almost keeps constant. When T is small and starts to increase, the gradually enlarged circular trajectory ensures the mobility of the UAV, which leads to a better result. However, if T is not large enough and the UAV has

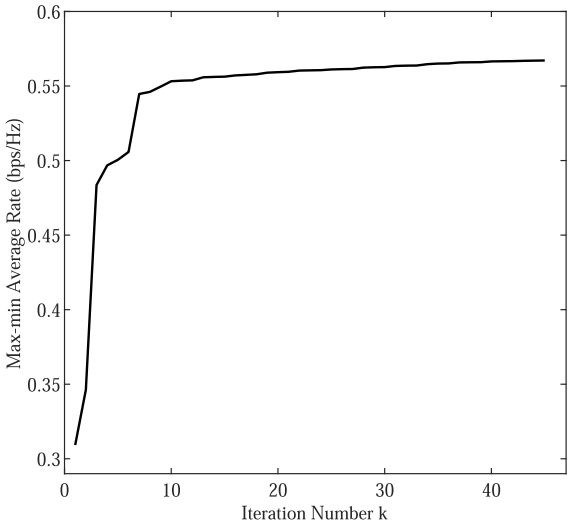

FIGURE 7. The convergence behavior of our proposed algorithm when T = 200s.

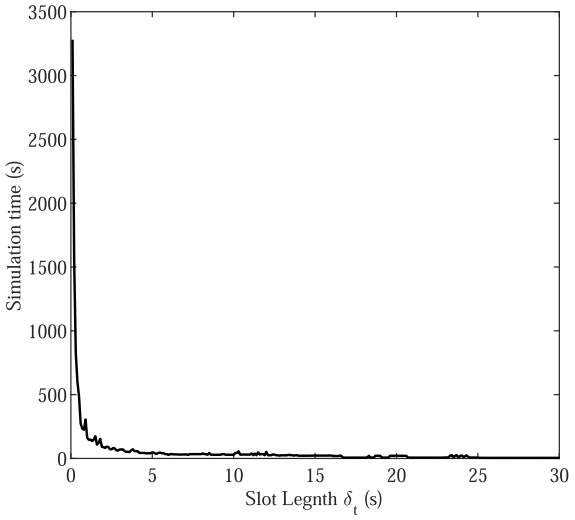

FIGURE 8. The simulation time versus slot length δ_t when T = 50s.

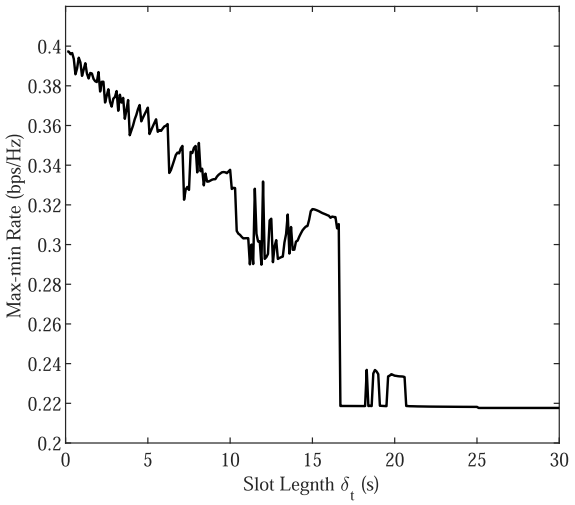

FIGURE 9. The max-min average user rate versus slot length δ_t when T = 50s.

too long total flying distance, the UAV will waste much time to complete it, and then the result decreases. Finally, the predesigned trajectory will be fixed when T is quite large. The speed of the UAV will decrease and go down to zero, when $T \to \infty$, to complete the fixed path within an ample time, which destroys the mobility of the UAV and leads to a worse result.

The drawback of algorithm 5 lies in the fact that it cannot efficiently use the time T. When T is small, its performance increases with the increasing T. When T is large enough, the optimized trajectory and power allocation results compromise with the preassigned nodes scheduling results, which leads to the degraded performance since algorithm 5 cannot fully use the distribution information of all nodes and the time T. For instance, even if the UAV stays at the top of a node, it still always communicates with all nodes rather than sometimes only communicates with that node, and this behavior takes a bad effect in the performance. The max-min average user rate of algorithm 6 is independent of mission completion time T since the UAV stays static, and channels among all nodes do not change. The UAV also does not fully use its mobility, and the distributions of nodes, which leads to the worst performance. Therefore, based on these benchmark schemes, the effectiveness of our proposed algorithm can be guaranteed since our proposed algorithm is composed of three algorithms which solve their respective subproblems, and we have verified the performance of these three algorithms, respectively.

Fig.7 shows that our proposed algorithm converges in about 45 iterations when T = 200 s. The convergence behavior is similar for different powers and T. In Fig.7, the optimized result almost keeps constant around k = 10, which means that our proposed algorithm can get good enough results with 3-4 blocks' iterations, which is fast and good enough. The simulation result also indicates that our proposed algorithm is monotonically increasing, which coincides with the convergence analysis result.

Fig.8 and Fig.9 show the relationship between the computation speed (complexity) and the precision of our proposed algorithm by changing δ_t. The number of N (the total number of time slots) decreases with the increasing δ_t, which accelerates our simulation speed but leads to degraded performance for a given T. When δ_t is too large, the assumption of the time discretization method which the UAV should approximately keep unchanged within any time slot, even at the maximum speed $V_{\max}$, will become invalid.

There are some discontinuity points in Fig.9, which are due to the approximation of N. In our simulation, we round $N = \frac{T}{\delta_t}$ down, and then different δ_t will possibly produce different N for a given T, which leads to the fluctuant curve in Fig.9. The most obvious discontinuity point in Fig.9 is located around $\delta_t = 17$, where N decreases from three to

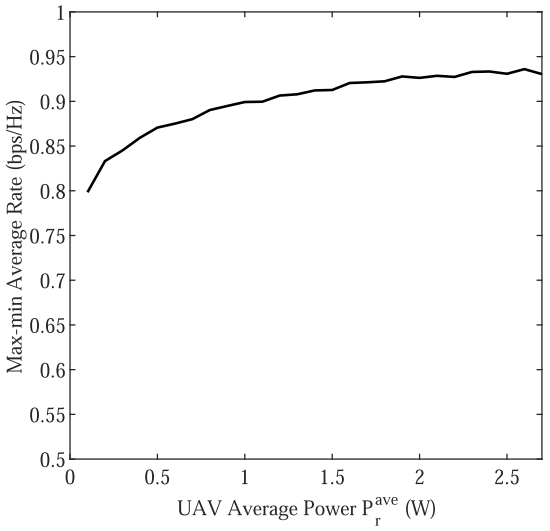

FIGURE 10. The max-min average user rate versus UAV average power P_r^{ave} when T = 300s.

two. Our problem then becomes a fixed location optimization problem, which is similar to algorithm 6 in Fig.5. The main difference is that the fixed point in our problem still changes with δ_t due to $r_2 = \frac{V_{\max} N \delta_t}{2\pi}$. r_2 increases with the increasing δ_t due to the approximation of N for a given T, which may be useful since it can enlarge the UAV initial trajectory when T is small. When δ_t is larger than 25, N will be equal to one, and our problem is equivalent to algorithm 6 in Fig.5. According to those two figures, we use $\delta_t = 1$ when T is small; otherwise, $\delta_t = 5$ in our simulation, which lets our algorithm be accurate enough with the acceptable complexity.

Fig.10 shows the influence of P_r^{ave} with fixed $P_s^{ave} = 0.5\ W$, $P_s^{max} = 2.5\ W$, and $P_r^{max} = 5 * P_r^{ave}$. The system output increases with the increasing UAV power, but the growth rate decreases. The UAV uses higher power to break the performance bottleneck caused by its limited and insufficient power supply compared to any GBS, to get better performance. However, when the UAV power is large enough, the limited GBSs' powers and the distance between GBSs and the UAV will be the performance bottleneck.

VII. CONCLUSION

In this paper, we investigate a UAV-enabled relaying system, where we use a mobile UAV relay to help some ground base stations send information to ground users periodically. Moreover, we solve a derived non-convex mixed-integer optimization problem to maximize the minimum average user rate by using block coordinate descent and successive convex approximation techniques, and jointly optimizing the UAV trajectory, nodes scheduling, and power allocation. Simulations show the effectiveness of our algorithm, some useful trade-offs and insights about the structure of our optimized trajectory, and the influence of two widely used trajectory initialization methods. We also hope that this paper can provide insights into the new UAV initial trajectory design since fully utilizing the distributions of nodes with different abilities (total available resources, heights, locations) is crucial for the performance optimization.

ACKNOWLEDGMENT

The author would like to thank to his supervisors Prof. Zengping Chen and Dr. Zhijin Wen, for their support in this paper. He is also indebted to Prof. Rui Zhang and Dr. Qingqing Wu for their assistance in the system model construction during his stay at the National University of Singapore. Moreover, he would also like to thank the anonymous referees for their comments which significantly improve the quality of the manuscript.

REFERENCES

[1] A. F. B. Hanscom and M. A. Bedford, "Unmanned aircraft system (UAS) service demand 2015–2035, literature review & projections of future usage," Res. Innov. Technol. Admin., U.S. Dept. Transp., Washington, DC, USA, Tech. Rep. DOT-VNTSC-DoD-13-01, 2013.

[2] Y. Zeng, Q. Wu, and R. Zhang, "Accessing from the sky: A tutorial on UAV communications for 5G and beyond," 2019, *arXiv:1903.05289*. [Online]. Available: https://arxiv.org/abs/1903.05289

[3] S. Zhang, Y. Zeng, and R. Zhang, "Cellular-enabled UAV communication: A connectivity-constrained trajectory optimization perspective," *IEEE Trans. Commun.*, vol. 67, no. 3, pp. 2580–2604, Mar. 2019.

[4] A. Al-Hourani, S. Kandeepan, and S. Lardner, "Optimal LAP altitude for maximum coverage," *IEEE Wireless Commun. Lett.*, vol. 3, no. 6, pp. 569–572, Dec. 2014.

[5] J. Lyu, Y. Zeng, R. Zhang, and T. J. Lim, "Placement optimization of UAV-mounted mobile base stations," *IEEE Commun. Lett.*, vol. 21, no. 3, pp. 604–607, Mar. 2017.

[6] R. Fan, J. Cui, S. Jin, K. Yang, and J. An, "Optimal node placement and resource allocation for UAV relaying network," *IEEE Commun. Lett.*, vol. 22, no. 4, pp. 808–811, Apr. 2018.

[7] P. Li and J. Xu, "UAV-enabled cellular networks with multi-hop backhauls: Placement optimization and wireless resource allocation," in *Proc. IEEE Int. Conf. Commun. Syst. (ICCS)*, Chengdu, China, Dec. 2018, pp. 110–114.

[8] L. Li, T.-H. Chang, and S. Cai, "UAV positioning and power control for two-way wireless relaying," *IEEE Trans. Wireless Commun.*, to be published.

[9] Y. Zeng, R. Zhang, and T. J. Lim, "Throughput maximization for UAV-enabled mobile relaying systems," *IEEE Trans. Commun.*, vol. 64, no. 12, pp. 4983–4996, Dec. 2016.

[10] J. Zhang, Y. Zeng, and R. Zhang, "Spectrum and energy efficiency maximization in UAV-enabled mobile relaying," in *Proc. IEEE Int. Conf. Commun. (ICC)*, Paris, France, May 2017, pp. 1–6.

[11] E. Frew and T. Brown, "Airborne communication networks for small unmanned aircraft systems," *Proc. IEEE*, vol. 96, no. 12, pp. 2008–2027, Dec. 2008.

[12] S. Zhang, H. Zhang, Q. He, K. Bian, and L. Song, "Joint trajectory and power optimization for UAV relay networks," *IEEE Commun. Lett.*, vol. 22, no. 1, pp. 161–164, Jan. 2018.

[13] H. Tu, J. Zhu, and Y. Zou, "Optimal power allocation for minimizing outage probability of UAV relay communications," 2019, *arXiv:1905.00543*. [Online]. Available: https://arxiv.org/abs/1905.00543

[14] Q. Wang, Z. Chen, H. Li, and S. Li, "Joint power and trajectory design for physical-layer secrecy in the UAV-aided mobile relaying system," *IEEE Access*, vol. 6, pp. 62849–62855, 2018.

[15] J. Fan, M. Cui, G. Zhang, and Y. Chen, "Throughput improvement for multi-hop UAV relaying," *IEEE Access*, vol. 7, pp. 147732–147742, 2019.

[16] J. Lyu, Y. Zeng, and R. Zhang, "UAV-aided offloading for cellular hotspot," *IEEE Trans. Wireless Commun.*, vol. 17, no. 6, pp. 3988–4001, Jun. 2018.

[17] Z. Xue, J. Wang, G. Ding, H. Zhou, and Q. Wu, "Cooperative data dissemination in air-ground integrated networks," *IEEE Wireless Commun. Lett.*, vol. 8, no. 1, pp. 209–212, Feb. 2019.

[18] M. Hua, Y. Wang, C. Li, Y. Huang, and L. Yang, "Energy-efficient optimization for UAV-aided cellular offloading," *IEEE Wireless Commun. Lett.*, vol. 8, no. 3, pp. 769–772, Jun. 2019.
[19] F. Cheng, S. Zhang, Z. Li, Y. Chen, N. Zhao, F. R. Yu, and V. C. M. Leung, "UAV trajectory optimization for data offloading at the edge of multiple cells," *IEEE Trans. Veh. Technol.*, vol. 67, no. 7, pp. 6732–6736, Jul. 2018.
[20] Q. Wu, Y. Zeng, and R. Zhang, "Joint trajectory and communication design for multi-UAV enabled wireless networks," *IEEE Trans. Wireless Commun.*, vol. 17, no. 3, pp. 2109–2121, Mar. 2018.
[21] J. Zhang, Y. Zeng, and R. Zhang, "UAV-enabled radio access network: Multi-mode communication and trajectory design," *IEEE Trans. Signal Process.*, vol. 66, no. 20, pp. 5269–5284, Oct. 2018.
[22] H. Wang, J. Wang, G. Ding, J. Chen, Y. Li, and Z. Han, "Spectrum sharing planning for full-duplex UAV relaying systems with underlaid D2D communications," *IEEE J. Sel. Areas Commun.*, vol. 36, no. 9, pp. 1986–1999, Sep. 2018.
[23] X. Jiang, Z. Wu, Z. Yin, W. Yang, and Z. Yang, "Trajectory and communication design for UAV-relayed wireless networks," *IEEE Wireless Commun. Lett.*, vol. 8, no. 6, pp. 1600–1603, Dec. 2019.
[24] A. Merwaday and I. Guvenc, "UAV assisted heterogeneous networks for public safety communications," in *Proc. IEEE Wireless Commun. Netw. Conf. Workshops (WCNCW)*, New Orleans, LA, USA, Mar. 2015, pp. 329–334.
[25] *Study on Enhanced LTE Support for Aerial Vehicles*, document TR 36.777, 3GPP, Sophia Antipolis, France, Jun. 2018. [Online]. Available: https://www.3gpp.org/ftp/Specs/archive/36_series/36.777/
[26] M. Mozaffari, W. Saad, M. Bennis, and M. Debbah, "Unmanned aerial vehicle with underlaid device-to-device communications: Performance and tradeoffs," *IEEE Trans. Wireless Commun.*, vol. 15, no. 6, pp. 3949–3963, Jun. 2016.
[27] D. W. Matolak and R. Sun, "Air–ground channel characterization for unmanned aircraft systems—Part I: Methods, measurements, and models for over-water settings," *IEEE Trans. Veh. Technol.*, vol. 66, no. 1, pp. 26–44, Jan. 2017.
[28] C. You and R. Zhang, "3D trajectory optimization in Rician fading for UAV-enabled data harvesting," *IEEE Trans. Wireless Commun.*, vol. 18, no. 6, pp. 3192–3207, Jun. 2019.
[29] M. Grant, S. Boyd, and Y. Ye. (Dec. 2018). *CVX: MATLAB Software for Disciplined Convex Programming, Version 2.1*. [Online]. Available: http://cvxr.com/cvx
[30] S. Boyd and L. Vandenberghe, *Convex Optimization*. Cambridge, U.K.: Cambridge Univ. Press, 2004.

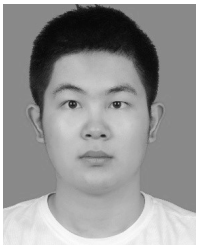

QINBO CHEN received the B.Eng. degree in communication engineering from Xidian University, in 2015, and the M.Eng. degree in information and communication engineering from Sun Yat-sen University, in 2018, where he is currently pursuing the Ph.D. degree with the School of Systems Sciences and Engineering. His research interests include convex optimization, UAV communications, and wireless communication.